



Design of an elevated pressure electrochemical flow cell for CO₂ reduction

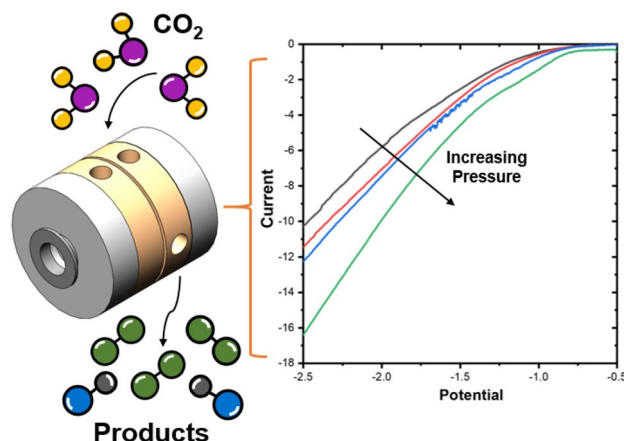
Andrew R. T. Morrison^{1,2,3} · Nandalal Girichandran¹ · Quincy Wols¹ · Ruud Kortlever¹

Received: 30 January 2023 / Accepted: 12 May 2023 / Published online: 27 May 2023
© The Author(s) 2023

Abstract

The electrochemical CO₂ reduction reaction (CO₂RR) has been proposed as a sustainable way of closing the carbon cycle while synthesizing useful commodity chemicals. One of the possible routes to scale up the process is the elevated pressure CO₂RR, as this increases the concentration of the poorly soluble CO₂ in aqueous systems. Yet, there are not many studies that focus on this route owing to the inherent challenges with high pressure systems. In this study, a novel high pressure flow cell setup has been designed and validated. The modular design uses a clamp system, which facilitates simple stacking of multiple cell parts while being capable of handling pressures up to 50 bar. The effects of CO₂ pressure on the reaction were investigated on a gold (Au) foil cathode in a 0.1 M KHCO₃ electrolyte. We successfully measured gaseous products produced during high pressure operation using an inline gas chromatograph. We find that the selectivity toward CO₂ reduction products is enhanced while that of H₂ evolution is suppressed as the pressure is increased from 2 to 30 bar. The reported setup provides a robust means to conduct high pressure electrolysis experiments in an easy and safe manner, making this technology more accessible to the electrochemical CO₂RR community.

Graphical abstract



Keywords Electrocatalysis · CO₂ electroreduction · High pressure CO₂ · Reactor design

1 Introduction

With climate change and global warming becoming an obvious reality, there is widespread agreement that immediate action is needed to control greenhouse gases emissions. One of the primary greenhouse gases is carbon dioxide (CO₂), a highly stable and therefore difficult molecule to break

Andrew R. T. Morrison and Nandalal Girichandran have contributed equally to this work.

Extended author information available on the last page of the article

down. However, under the right conditions there are routes to reduce CO₂ and generate valuable hydrocarbons that can be used as fuel or feedstock for further processing [1]. CO₂ can be converted to other chemicals in a variety of processes utilizing thermochemical devices (e.g., reverse water–gas shift reactors) [2–5] or through bioreactors [6]. However, one of the most promising routes is the electrochemical CO₂ reduction reaction (CO₂RR). This process directly utilizes electrical energy to convert CO₂ into useful chemicals and has the potential to be completely sustainable by deriving energy directly from renewable sources like solar, wind, and geothermal [7].

The CO₂RR has been well studied at the laboratory scale. The developed understanding of reaction mechanisms [8–11] have allowed significant strides to be made in catalyst development. However, the large-scale industrial deployment of the CO₂RR is hindered by several factors including, but not limited to, the poor solubility of CO₂ that creates mass transfer limitation and lowers reaction rates, poor product selectivities, and unstable electrocatalysts [12, 13]. Development of catalysts have made several important advances in H-cell type experimental configurations. However, different configurations are required because the H-cell is not an appropriate environment to test catalysts for commercial application where typically, 200 mA/cm² partial current density of product is required [14, 15]. Moreover, besides the choice of electrocatalyst, factors such as the electrolyzer design, electrolyte choice, and optimal operating conditions (pH, temperature, pressure, mass transport conditions) play a crucial role in determining the outcome of the reaction [16–20]. Therefore, there is a need to examine the CO₂RR under more combinations of conditions that are likely to be encountered in scalable and industrially relevant electrolyzers, and to test electrocatalytic materials under these operating conditions.

Due to the low solubility of CO₂ in aqueous electrolytes, delivering sufficient CO₂ to the surface of the electrode to avoid mass transport limitations is pivotal for operating CO₂RR at industrial scales. Currently, there are several reactor designs that solve this problem, the most popular being the gas diffusion electrode (GDE) based electrolyzers, which deliver gaseous CO₂ through the porous GDE to the catalysts layer that in turn is in contact with the liquid electrolyte [21, 22]. Electrolyzer designs such as Taylor flow cells [23], or porous electrode cells [24] use a similar concept by providing gaseous CO₂ as directly as possible to the catalyst sites (thereby not depending on dissolved CO₂ from the bulk of the electrolyte). These technologies solve the issue of poor CO₂ solubility by increasing the effective speed of diffusion of CO₂. Alternately, the concentration of CO₂ in the electrolyte can be increased. This can be done by either using non-aqueous electrolytes with higher CO₂ solubilities [16, 25, 26] or pressing more CO₂ into the solution by applying an elevated CO₂ pressure [27]. Elevated pressure electrolyzers

have been mentioned as one of the more promising routes to industrialize the CO₂RR [28]. These are two different approaches to CO₂RR reactors. In the GDE design CO₂ can be delivered to (near) the electrode as a gas, and the electrode is a porous membrane assembly. In contrast the high pressure systems operate with two parallel plate electrodes, and CO₂ is delivered dissolved in the electrolyte. Despite the promise of this type of reactor design, the amount of studies that focus on high pressure CO₂RR is very limited in comparison to GDE based electrolyzers. A possible explanation for this is the challenges that working at elevated pressure poses to the average laboratory team. Here, we report the design of a modular elevated pressure CO₂RR reactor, which can serve as a guide to explore this promising field.

Studying the CO₂RR at elevated pressure has a long history [29], and the reactors in previous work on the subject can be divided into two categories: autoclave reactors [30–32], and larger scale flow cells [33–39]. The autoclave reactors are essentially normal laboratory scale electrochemical H-cells or three electrode cells put into a pressurized box. These cells generally have reference electrodes and are operated fully in batch mode with small electrode areas. They have been used to find very high faradaic efficiencies toward both CO, formate and C₂₊ chemicals, dependent on catalyst choice [30, 31, 40]. Importantly, they have also been used to demonstrate the potential capability of elevated pressure CO₂RR to deliver on the requirements for a commercial electrolyzer, that is 200 mA/cm² partial current density. The larger scale flow cells represent a more industrial kind of reactor and were used to answer questions regarding the scaling up of elevated pressure CO₂ electrolyzers. The electrode areas are significantly larger than with the autoclave reactors, with most studies using at least a tenfold higher electrode surface area. The flow cells universally do not have reference electrodes and are operated galvanostatically, which makes it difficult to compare product selectivities and production rates with other systems. Additionally, since the product selectivities and reaction rates are so potential dependent in the CO₂RR, these cells designs can only give limited fundamental insight into the CO₂RR at elevated pressures. A table summarizing the characteristics and obtained results with a few other elevated pressure cells from literature can be found in the supplementary information (see S5 in the SI). High faradaic efficiencies (FE) were obtained in these cells, but the current densities of the most successful autoclave style cells have never been reached in parallel plate flow reactors (200 mA.cm⁻² for autoclave and < 50 mA.cm⁻² for larger flow cells). This shows that scaling up of high pressure CO₂ electrolyzers is not straightforward.

The difficulty in scaling from a small autoclave cell to a large industrial-style cell presents a clear need for an intermediary type of reactor. Furthermore, the challenges in achieving the same order of magnitude current densities in

large flow cells as where observed in autoclave cells shows there are parameters of the design which have not been fully understood. The only way to study these parameters is by making a laboratory version of such a cell. Such a flexible flow reactor of moderate size with a reference electrode can yield information about how to scale up the elevated pressure CO₂RR. Here, we report on the design of a modular, laboratory size CO₂RR flow reactor and will demonstrate its performance for CO₂RR experiments at elevated pressures. First, the design of the cell is discussed with a special focus on the areas where high pressure presents an interesting design challenge, then the electrochemical behavior of the reactor is verified, and finally the product characterization capability.

2 Experimental section

2.1 Materials

Potassium bicarbonate (KHCO₃, ≥ 99.95% trace metals basis, 99.7–100.5% dry basis) was used to prepare both a 0.1 M KHCO₃ anolyte and catholyte. The working electrode used for electrochemical experiments was a gold foil cathode (99.9%, Mateck GmbH) and IrMMO coated titanium foil [41, 42]) (MAGNETO special anodes B.V, The Netherlands) was used as the counter electrode. Nafion 117 (Ion Power GmbH) was cleaned in MilliQ water and used as the ion exchange membrane. For testing the reference electrode potential versus pressure, a solution of 0.01 M of K₄Fe(CN)₆·3H₂O (≥ 99.95% trace metals basis, Sigma Aldrich) and 0.05 M of KNO₃ (ACS reagent, ≥ 99.0%, Sigma Aldrich) was used as standard. An ultrapure water purification system (MilliQ IQ 7000, Merck–Millipore, USA) was used as water source for all experiments. All reagents were used without further purification.

2.2 Electrochemical measurements

Electrochemical experiments were conducted using a Bio-Logic SP300 dual-channel potentiostat with EIS analyzer. 1 cm² electrodes were secured in place by creating slots in stainless steel endplates (see section S1 in supplementary for schematic). The PEEK flow plates for the anolyte and catholyte have an internal volume of (−0.79 cm³). Nafion 117 served as the separator between the two chambers. For all experiments, a miniaturized leakless Ag/AgCl reference electrode (LF 1.6–45 mm, Innovative Instruments, Inc., USA) was used as the reference electrode. The body of the electrode houses the silver wire in a peek tube and the junction at the end is described by the manufacturer as non-porous and conductive. The tip at the head is a gold plated connector. The reference electrode was carefully stored in a 3.5 M KCl solution between

experiments and its potential was carefully monitored against a master reference electrode. Since the performance of these electrodes is unknown at elevated pressure, we performed experiments to test their stability at 2, 5, 10, 15, 20, 25, and 30 bar. All potentials are reported versus Ag/AgCl electrode. Experiments were all conducted at 30 bar or less for safety reasons, although the system was pressure tested up to 50 bar. CO₂RR experiments were conducted at different pressures (2, 5, 15, and 30 bar) by applying a constant current of 10 mA/cm² in order to validate the system. The apparatus is sized for operation up to 200 mA/cm², but this lower current density is selected as a tradeoff between testing the system at a stable, well characterized regime and the desire for high current density. The cell resistance was monitored by carrying out a potentiostatic electrochemical impedance spectroscopy (see Supplementary Information, S2).

2.3 Product analysis

An inline gas chromatograph (CompactGC 4.0, Global Analyzer Solutions, The Netherlands) was used to measure the gaseous products synthesized during the reaction. Gas cylinders (Linde Gas Benelux B.V., The Netherlands) containing custom gas mixtures of different product gases with a range of 50–8000 ppm in CO₂ were used to calibrate the GC. The gas products were analyzed every 2 min. The GC consists of 2 TCD detectors (one each for CO and H₂) and an FID detector to analyze hydrocarbons (C₁–C₆). The FID channel is comprised of an Rtx-1, 5.00 μm (15 m * 0.32 mm) analytical column, the first TCD channel consists of a Carboxen 1010 (3 m * 0.32 mm) pre-column and a Molsieve 5A (5 m * 0.32 mm) analytical column, and the second TCD channel consists of a Carboxen 1010 (3 m * 0.32 mm) pre-column and a Molsieve 5A (7 m * 0.32 mm) analytical column. They help in the separation of the components before entering the respective channel detectors.

HPLC (Agilent Technologies 1260 Infinity, USA), was used for the analysis of liquid products collected after the completion of the reaction. Standard solutions of the desired chemicals (formic acid > 98%, Sigma-Aldrich, USA) were used for the calibration with dissolutions ranging from 0.1 to 50 mM (see section S6 of the supplementary information). 5 μL of the product sample was injected into a series of Aminex HPX-87H columns (Biorad) which were heated to a temperature of 60 °C using a 1 mM H₂SO₄ solution as eluent. A Refractive Index Detector (RID) was used for the detection of the products.

3 Results and discussion

3.1 Apparatus design

The goal of the designed and reported setup is to enable the study of the CO₂RR at different pressures in a cell that can be used to study parameters important for scaling up electrolyzer design, while being at a more manageable lab scale. Simultaneously, the design will combine operation at elevated pressure with characterization capabilities typical for a normal lab cell—potential measurement via a reference electrode and product characterization via gas chromatography at time scales not significantly different than a standard experiment.

A schematic of the design of the entire system can be found in Fig. 1. The reactor is a membrane-separated parallel plate flow cell with two pressurized external reservoirs. The electrolyte is pumped from the reservoir to the reactor, through a back pressure regulator, and then back into the external reservoir at a flow rate 25 ml/min. Gas is pressurized into the reservoir at a controlled rate through a pressure controller (Bronkhorst High-Tech BV, The Netherlands, and Pressure Control Solutions BV), and the gas outlet is directed to the inline GC. Thus, CO₂ consumed in the reactor is continuously replaced by the gas inlet. Several design

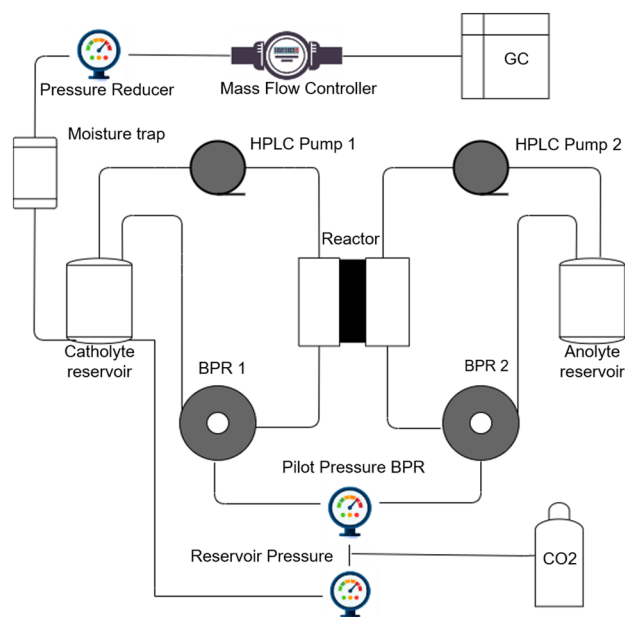


Fig. 1 A schematic of the piping for the experimental setup created here to study the CO₂RR at elevated pressures. The system consists of the reactor which has two compartments separated by a membrane, both of which have electrolyte constantly feed into them from separate reservoirs, and a line from the catholyte reservoir into a gas chromatograph for inline product analysis. The pressures of the reactor and the two reservoirs can be controlled independently

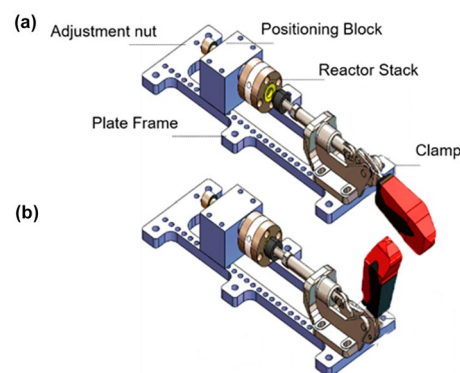


Fig. 2 Renderings of mechanical drawings of the reactor and compression system. The system is easy to assemble and disassemble, facilitated by the clamped design, and different segments can be easily added to the reactor stack as required. **a** Open position, **b** Closed position of the clamp

choices are discussed below, and for detailed schematic drawing of the reactor please see section S1 of the supplementary information.

3.2 Reactor assembly design

A notable element of the design of the reactor is the clamp system for containing the pressure in the reactor, inspired by Branch et al. [43] (See Fig. 2). From the authors' experience, the style of reactor that relies on nuts and bolts to contain the pressure (or just the electrolyte for atmospheric cells) is extremely time-consuming. In this regard, the clamp element of the design significantly increases the speed of assembly of the reactor. The turnaround time for experiments is extremely important because it will directly influence how many experiments can be performed on an apparatus. The clamp design also allows for flexibility in cell design. If the end plates have adaptors for the linear bearings and the size is compatible, any cell can be inserted into the clamp system and have its pressure contained.

3.3 Reference electrode

The lack of reference electrodes (REs) in high pressure CO₂ electrolyzers indicates that there is a major challenge with adding them to these systems. Indeed, there are costly (compared to standard REs) commercial options available that are meant to be appropriate REs for high pressure systems. The major challenge that justifies the increased costs is the gases dissolved in the electrolyte at high pressure. If the gases infiltrate the reference electrode and the system is depressurized too quickly the gases do not have time to escape, and they can damage the frit or the casing of the electrode. However, the best solution is that high pressure gases are not allowed to penetrate inside the RE in the first place. For this

reason, we tested “leak-free” REs, that showed to avoid these issues at pressures tested here. In order to check the performance and stability, the leak-free Ag/AgCl RE was tested before and after each experiment with respect to a master RE. Open Circuit Voltage (OCV) measurements were carried out to check if the drift in potential was within acceptable limits (max variation $\leq 2\text{--}3$ mV) [44]. Even though it is difficult to predict how much drift in potential will occur after each experiment, it is wise to monitor this in order to ensure the electrode’s proper functioning (especially, at higher pressures).

3.4 Pressure regulation

The design of the pressure regulation system has many components that must be considered. For the system to be an elevated pressure CO₂ electrolyzer it must be able to deliver electrolyte saturated with CO₂ at a controllable pressure to the cathode surface. This means there will be a part of the system to dissolve CO₂ at the required pressure and transport it to the cathode. Pressing CO₂ into the electrolyte is accomplished by a pressure chamber, but keeping the reactor pressurized presents a slightly different challenge because the system accommodates a divided reactor with a membrane separating catholyte and anolyte. If the pressure is unbalanced, then the membrane will break or stretch and contact one of the electrodes. Therefore, either a mechanically reinforced membrane must be used, possibly hampering the other important properties of the membrane or the pressure must be balanced. Here, we opted for a dual back pressure regulator in the system. These ensure a balanced pressure across the membrane as long as the electrolyte is flowing. This is accomplished by piloting the dual back pressure regulator under the same pressure, which means they will enforce the same back pressure at their inlets. The dual back pressure regulator also allows for independent control of the pressure in the reactor and the pressure reservoir. Thus, allowing the separation of the effects of mechanical and gaseous pressure on the CO₂RR. It also allows the reactor to be kept at a pressure high enough to prevent the degasification of the electrolyte in a reactor that is hotter than the reservoir (due to resistive heating at high current density), which will decrease the solubility of CO₂ locally.

3.5 Reservoir sizing

There is a trade-off in deciding the size of the external reservoir. A smaller reservoir will result in more accurate HPLC measurements for quantification of liquid products. A larger reservoir is necessary for longer operating times so that the consumption of water for the CO₂RR does not significantly concentrate the electrolyte over the course of the experiment. Further, in both cases the gas headspace of the reservoir

must be minimized to equilibrate GC measurements as quickly as possible. The reservoir was therefore designed to be flexible. In this work it was configured to have 20 ml of electrolyte in total (including electrolyte in the reactor and tubing) to favor longer operation and because quantification of liquid products was less important for these tests. With 20 ml of electrolyte the reactor can continuously operate for 2.5 days at 200 mA/cm² before it consumes 5% of the water in the system. The gas headspace used was 2 ml. Since there are no trade-offs for the gas headspace, this represents the smallest volume which avoided liquid entering the pathway to the GC.

3.6 Pump sizing

The options for pumps that operate in the desired pressure range are relatively small at flow rates interesting in laboratory experiments. There are two factors to consider when selecting pump size. First, the diffusion layer thickness—faster pumping can lead to a thinner diffusion layer and thus faster CO₂RR. To meaningfully study this parameter requires a combination of a very fast pump and a cell with a low volume. The second factor to consider is the rate of consumption of CO₂ in the reactor. In the ideal scenario, at the upper end of the pump’s range, the CO₂ concentration of the electrolyte leaving the reactor will be within some factor of the concentration of CO₂ of the electrolyte entering the reactor at the current densities of interest. Then the pump’s operational range will cover the area where this effect can be studied well. The pump speed in this work was selected to consider the latter effect because the pump rates to effect diffusion layer thickness are large. The pumps selected are capable of pump speeds up to 50 ml/min, but 25 ml/min during long term operation. At the maximum continuous pumping rate this will be able to keep the CO₂ concentration in the electrolyte in the reaction chamber at more than 95% of the reservoir concentration for currents lower than 500 mA/cm² at pressures of 5 bar and up, allowing for a wide range of operation before consuming the CO₂ in the reactor becomes an issue.

3.7 General operation

The reactor performs well and as expected in general function. Notably, the clamp system is successful in minimizing the turnaround time of experiments. The time to depressurize, disassemble, exchange electrolyte, and reassemble was, at quickest, half an hour, which is superior to several atmospheric cell designs and significantly better than other pressurized systems. The system was pressure tested with hydrostatic pressure up to 50 bar, the eventual desired pressure range, so it will function up to that pressure even

though in the following experiments pressures were limited to 30 bar or less.

3.8 Effect of pressure on reference electrode potential

The RE's functioning was tested in a solution of 0.01 M $\text{K}_4\text{Fe}(\text{CN})_6 \cdot 3\text{H}_2\text{O}$ and 0.05 M KNO_3 . Figure 3 is a plot of the peak potential of ferrocyanide oxidation versus the reactor pressure (mechanical pressure) and Fig. 4 displays the equilibrium potential vs. the reservoir pressure (gas pressure). In both cases there is less than 10 mV drift in potential as pressure above atmospheric is first applied for both mechanical and gas pressure. The potential of the RE first creeps upwards before stabilizing after the pressure reaches 10 bar, for both the reactor and reservoir pressure. Figures 3 and 4 show that the RE potential does not depend on the applied pressure, either mechanical pressure or with dissolved gases, as otherwise there would be a difference in the way that pressure affects these two sets of potentials. No instabilities or potential drifts due to the earlier mentioned crossover of dissolved gasses into the RE were observed. Therefore, the leak-free RE works as it is supposed to and can be used in elevated pressure experiments.

3.9 Electrochemical measurements

Electrochemical tests were performed at several different pressures and across a wide range of electrode voltages. Figure 5 displays the linear sweep voltammograms (LSV) of a polycrystalline Au foil electrode in a 0.1 M KHCO_3 electrolyte at different CO_2 pressures. As shown, increasing the pressure leads to an increase in current density across

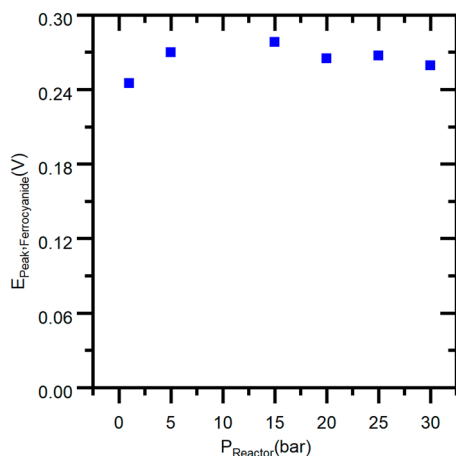


Fig. 3 Reactor pressure versus peak potential of 0.01 M ferrocyanide oxidation in 0.05 M potassium nitrate. There is a very small increase in the potential from atmospheric pressure to 5 bar, but it is very stable at higher pressures

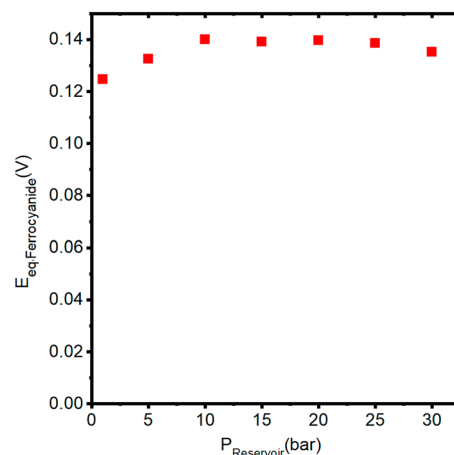


Fig. 4 Reservoir pressure versus equilibrium potential of 0.1 M ferrocyanide oxidation in 0.005 M potassium nitrate. There is a very small increase in the potential from atmospheric pressure to 10 bar, but it is very stable at higher pressures

all potentials, indicating a direct relationship between the CO_2RR and the concentration of CO_2 in the electrolyte. Similar behavior has been reported for a silver plate electrode in the work of Federica et al. [45], but without a RE.

The other important element of this experimental setup is product characterization. In order to test that aspect, chronopotentiometry was carried out at -10 mA cm^{-2} for different pressures (namely 2, 5, 15, and 30 bar) and the faradaic efficiencies of different products were measured. A current density of -10 mA cm^{-2} is specifically chosen as a typical current density observed in CO_2RR studies. The main importance of the experiments is to confirm that we can observe the pressure effect on the CO_2RR . Further optimization of the pressure effect is possible, as can be seen

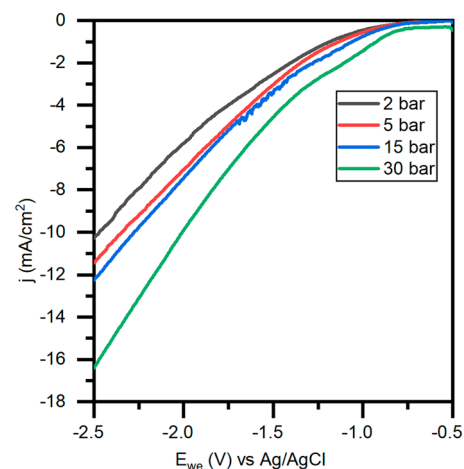


Fig. 5 LSV polarization curves at 10 mV s^{-1} on a Au foil electrode in a 0.1 M KHCO_3 electrolyte under applied CO_2 pressures of 2, 5, 15, and 30 bar. The current density increases as expected with pressure

elsewhere, but will be left for future work with this apparatus. The results of the experiments can be seen in Fig. 6. As expected, there is a positive relationship between pressure and the FE for the CO₂RR products while the HER is suppressed. The main products detected include H₂, CO, and formate. As shown, increasing the pressure from 2 to 30 bar decreased the selectivity of H₂ from about 60% to 20% while increasing the selectivity toward CO and formate, with the effect being most dramatic at lower applied pressures. This is expected because the concentration of CO₂ increases with a rise in pressure, leading to improved reactant availability and mass transport. Also notable in Fig. 6 and more importantly in terms of reactor design, at 5 bar there is 92% closure of the charge balance, which drops to 80% of charge accounted for at 30 bar. The drop in FE at the highest pressure is not completely explained in our data. However, the charge balance was certainly more difficult to close at higher pressure. Great care needed to be taken to eliminate leaks, since the effect of these is only magnified at high pressure. Additionally, a more stable pressure control system removed pressure oscillations which disrupted measurements more significantly at high pressures. Aside from these, there are other effects which can prevent closing the charge balance completely that are challenging to address: gas permeation (especially H₂) through the Nafion membrane or into the O-rings [46, 47], several C₂₊ products are more likely to form at higher pressure [27] but could be present below the quantification limit, and difficult to detect leaks may still be present. Even if each of these only makes up a couple percentage points, together they could explain the difference between the low pressure FE and the high pressure FE. Furthermore, even with the lower FE at high pressure, it is still a charge balance closure that is comparable with several benchmark works in the CO₂RR field [48–51].

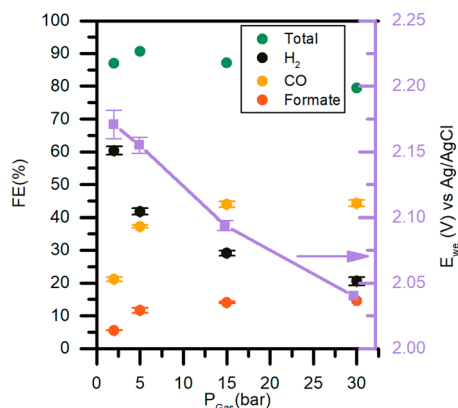


Fig. 6 Faradaic efficiencies (left axis) and potential (right axis) of carbon monoxide, hydrogen, formate, and the total FE on Au foil at a current density of 10 mA/cm² in a 0.1 M KHCO₃ electrolyte at applied CO₂ pressures of 2, 5, 15, and 30 bar

3.10 GC response time

One of the challenges of operating at high pressure is that it complicates inline GC measurements. The standard functioning of an inline GC involves sampling the headspace above an electrochemical cell at a constant flowrate into a GC [52]. Eventually the concentration in the headspace of the product molecules reaches an equilibrium which can be related to the production rate in the reactor. At elevated pressures the effective volume of the headspace will increase linearly with the pressure. The volume of headspace that is being sampled by the GC (in our case 2 ml, see Sect. “Reservoir sizing” above) is a key factor because of the dynamics that affect GC settling time (the time that it takes the GC signal to be within 5% of the actual concentration in the head space), given by:

$$t_s \approx \frac{3 \cdot V_{h_eff}}{q} \quad (1)$$

where t_s is the settling time, V_{h_eff} is the effective volume of headspace (Pressure \cdot V_h), and q is the flowrate of gas from the headspace to the GC. The settling time is thus determined by the flow rate of gas to the GC and the size of the headspace. As can be seen, increasing the pressure, which increases V_{h_eff} , linearly increases the settling time, up to 30 times longer at the highest pressure used here. The obvious solution is to increase the flowrate q to balance the effectively larger headspace, but this comes with a tradeoff. The final concentration of product in the headspace is given by:

$$C_{h_lim} = r/q \quad (2)$$

where C_{h_lim} is the limiting value of concentration of the product in the headspace and r is the production rate of the product in the reactor. This means that C_{h_lim} decreases linearly with q , which decreases the sensitivity with which the GC can measure concentration, and thus production rate. The other option is to decrease the volume of the headspace, but this quickly runs into physical constraints.

The solution to these issues is to modify the standard in-line GC procedure somewhat. The key observation is that the rate of change of C_h is highest when q is lowest (in absolute terms). Therefore, switching q from a low to high value during the experiment can decrease the settling time, without trading off sensitivity in GC measurements. An example of this procedure can be seen in Fig. 7. If 80% of C_{h_lim} is reached during the low q period, then the settling time can be reduced by 25%, and if 90% of C_{h_lim} is reached then settling time is reduced by 50%. For the details of these calculations, we redirect the interested reader to section S4 in the supplementary information. Thus, achieving reasonable settling times is possible with high pressure reactors, it however does require consideration of all the parameters.

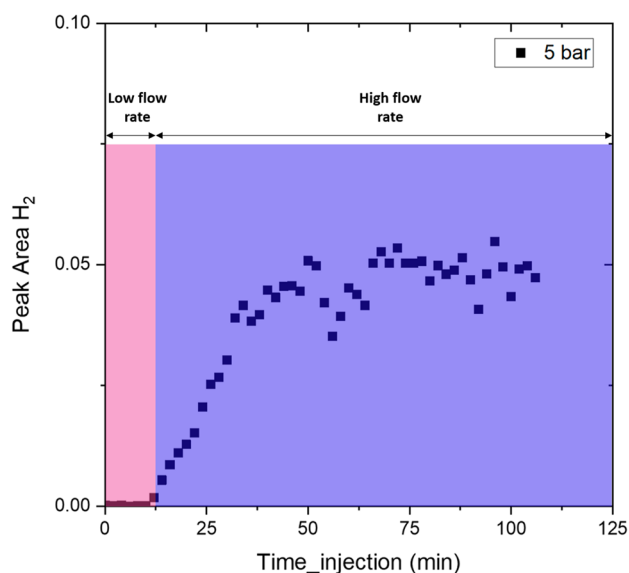


Fig. 7 A typical switched flow rate GC measurement. The low flow region at the start allows the concentration to quickly build up, while the high flow region at the end maintains the sensitivity of the GC measurement. The effect is to speed up the time it takes the GC measurements to stabilize. The buildup of concentration during the low flow is not seen at the GC due to the low linear velocity at low flow rates

3.11 Extended operation

There are several reasons why extended operation is interesting, including long term testing of electrodes and catalysts for degradation. One of the advantages of having an external reservoir of electrolyte is long continuous operation, as the CO₂RR will consume water molecules during operation, which will eventually change the concentration of the electrolyte. The system presented here is capable of operating for several hours continuously, as can be seen in Fig. 8.

4 Conclusion

We have demonstrated the successful design and operation of an elevated pressure divided CO₂RR flow cell to perform experiments that can be considered standard in the field. To achieve this design, minimization of pressure differentials across the dividing membrane by double back pressure regulators piloted by the same pressure was essential, as well as careful consideration of design parameters such as reservoir and pump sizing. The cell assembly/disassembly time was found to be faster than even some standard atmospheric designs, owing to the quick release clamp design to enclose the pressure inside the reactor (complete turnaround within a half hour).

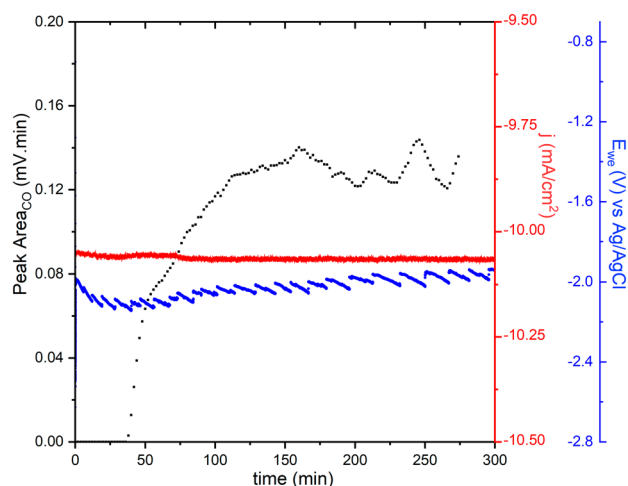


Fig. 8 An extended operation at 30 bar showing the stability of applied current, recorded potential and GC peak area for CO versus over time. The cell operates here for nearly 5 h at a current density of 10 mA cm⁻² (actual applied current density ~10.06 mA cm⁻²) and stable electrode potential and CO peak area (after an hour)

Electrochemically, the cell performed well and the leakless reference electrode provided a stable reference potential across a range of both reactor and reservoir pressures (stable within 10 mV between 1 and 30 bar). Standard electrochemical experiments, such as linear sweep voltammetry, were successfully performed. Product characterization by in-line GC was possible by utilizing a switching flow rate system, which greatly decreased the settling time, allowing faster measurements (stable readings reached within 60 min for lower pressures and within 100 min at the highest pressure). The FE for CO₂RR products dramatically increases from close to 26% at 2 bar to about 60% at 30 bar while H₂ is suppressed, and more importantly 85–90% of the charge balance was closed at lower pressure, dropping only to 82% at 30 bar which is still equivalent to several studies in the literature. The system explained here in detail is successful in its aims and configurable enough to be useful in studying a range of CO₂RR research questions relating to elevated pressure reactors like high current density or CO₂ conversion rate.

Supplementary Information The online version contains supplementary material available at <https://doi.org/10.1007/s10800-023-01927-7>.

Author contributions AM: Conceptualization, design, supervision, writing—original draft, editing. NG: Experiments, design, analysis, writing—original draft, editing. QW: Design, writing. RK: Conceptualization, supervision, writing—review & editing.

Funding This work was supported by RVO (Netherlands Enterprise Agency), TKI new gas and NWO (Netherlands Organization for Scientific Research) under TEEI116076, TCCU118009, TKI-2019-CCUS-SUPERHIPE, and Electrons to Chemical Bonds (E2CB).

Declarations

Competing interest All authors have given approval to the final version of the manuscript and declare no competing financial interests that could have influenced the work reported here.

Open Access This article is licensed under a Creative Commons Attribution 4.0 International License, which permits use, sharing, adaptation, distribution and reproduction in any medium or format, as long as you give appropriate credit to the original author(s) and the source, provide a link to the Creative Commons licence, and indicate if changes were made. The images or other third party material in this article are included in the article's Creative Commons licence, unless indicated otherwise in a credit line to the material. If material is not included in the article's Creative Commons licence and your intended use is not permitted by statutory regulation or exceeds the permitted use, you will need to obtain permission directly from the copyright holder. To view a copy of this licence, visit <http://creativecommons.org/licenses/by/4.0/>.

References

1. Pei Y, Zhong H, Jin F (2021) A brief review of electrocatalytic reduction of CO₂—materials, reaction conditions, and devices. *Energy Sci. Eng.* 7:1012–1032
2. Götz M, Lefebvre J, Mörs F, McDanielKoch A, Graf F, Bajohr S, Reimert R, Kolb T (2016) Renewable power-to-gas: a technological and economic review. *Renew. Energy* 85:1371–1390
3. Bailera M, Lisbona P, Romeo LM, Espatolero S (2017) Power to gas projects review: lab, pilot and demo plants for storing renewable energy and CO₂. *Renew. Sustain. Energy Rev.* 69:292–312
4. Perathoner S, Centi G (2014) A new scenario for green & sustainable chemical production. *J. Chin. Chem. Soc.* 61(7):719–730
5. Galadima A, Muraza O (2015) From synthesis gas production to methanol synthesis and potential upgrade to gasoline range hydrocarbons: a review. *J. Natural Gas Sci. Eng.* 25:303–316
6. Goli A, Shamiri A, Talaiekhosani A, Eshtiaghi N, Aghamohammadi N, Aroua MK (2016) An overview of biological processes and their potential for CO₂ capture. *J Environ Manage* 183:41–58
7. Brewis I, Shahzad R-F, Field RW, Jedidi A, Rasul S (2022) Combining experimental and theoretical insights for reduction of CO₂ to multi-carbon compounds. *Discov Chem Eng.* <https://doi.org/10.1007/s43938-022-00009-y>
8. Kortlever R, Shen J, Schouten KJP, Calle-Vallejo F, Koper MTM (2015) Catalysts and reaction pathways for the electrochemical reduction of carbon dioxide. *J. Phys. Chem. Lett.* 6(20):4073–4082
9. Hatsukade T, Kuhl KP, Cave ER, Abram DN, Jaramillo TF (2014) Insights into the electrocatalytic reduction of CO₂ on metallic silver surfaces. *Phys Chem Chem Phys* 16(27):13814–13819
10. Feaster JT, Shi C, Cave ER, Hatsukade T, Abram DN, Kuhl KP, Hahn C, Nørskov JK, Jaramillo TF (2017) Understanding selectivity for the electrochemical reduction of carbon dioxide to formic acid and carbon monoxide on metal electrodes. *ACS Catal* 7(7):4822–4827
11. Zhu M, Tian P, Li J, Chen J, Xu J, Han Y-F (2019) Structure-tunable copper–indium catalysts for highly selective CO₂ electroreduction to CO or HCOOH. *ChemSusChem* 12(17):3955–3959
12. Garg S, Li M, Weber AZ, Ge L, Li L, Rudolph V, Wang G, Rufford TE (2020) Advances and challenges in electrochemical CO₂ reduction processes: an engineering and design perspective looking beyond new catalyst materials. *R Soc Che* 8:1511–1544
13. Van Daele K, De Mot B, Pupo M, Daems N, Pant D, Kortlever R, Breugelmanns T (2021) Sn-based electrocatalyst stability: a crucial piece to the puzzle for the electrochemical CO₂ reduction toward formic acid. *ACS Energy Lett* 6(12):4317–4327
14. Jouny M, Luc W, Jiao F (2018) General techno-economic analysis of CO₂ electrolysis systems. *Ind Eng Chem Res* 57(6):2165–2177
15. Verma S, Kim B, Jhong H-RM, Ma S, Kenis PJA (2016) A gross-margin model for defining technoeconomic benchmarks in the electroreduction of CO₂. *Chemsuschem* 9(15):1972–1979
16. de SallesPupo MM, Kortlever R (2019) Electrolyte effects on the electrochemical reduction of CO₂. *ChemPhysChem* 20(22):2926–2935
17. Kas R, Kortlever R, Yılmaz H, Koper MTM, Mul G (2015) Manipulating the hydrocarbon selectivity of copper nanoparticles in CO₂ electroreduction by process conditions. *ChemElectroChem* 2(3):354–358
18. Gupta N, Gattrell M, MacDougall B (2006) Calculation for the cathode surface concentrations in the electrochemical reduction of CO₂ in KHCO₃ solutions. *J Appl Electrochem* 36(2):161–172
19. Weekes DM, Salvatore DA, Reyes A, Huang A, Berlinguette CP (2018) Electrolytic CO₂ reduction in a flow cell. *Acc Chem Res* 51(4):910–918
20. Endrődi B, Bencsik G, Darvas F, Jones R, Rajeshwar K, Janáky C (2017) Continuous-flow electroreduction of carbon dioxide. *Prog Energy Combust Sci* 62:133–154
21. Higgins D, Hahn C, Xiang C, Jaramillo TF, Weber AZ (2019) Gas-diffusion electrodes for carbon dioxide reduction: a new paradigm. *ACS Energy Lett* 4(1):317–324
22. Del Castillo A, Alvarez-Guerra M, Solla-Gullón J, Sáez A, Montiel V, Irabien A (2017) Sn nanoparticles on gas diffusion electrodes: synthesis, characterization and use for continuous CO₂ electroreduction to formate. *J CO₂ Utilization* 18:222–228
23. Zhang F, Chen C, Tang Y, Cheng Z (2020) CO₂ reduction in a microchannel electrochemical reactor with gas-liquid segmented flow. *Chem Eng J* 392(February):124798–124798
24. Vedharathinam V, Qi Z, Horwood C, Bourcier B, Stadermann M, Biener J, Biener M (2019) Using a 3D porous flow-through electrode geometry for high-rate electrochemical reduction of CO₂ to CO in ionic liquid. *ACS Catal* 9(12):10605–10611
25. Zhang X, Zhao Y, Hu S, Gliege ME, Liu Y, Liu R, Scudiero L, Hu Y, Ha S (2017) Electrochemical reduction of carbon dioxide to formic acid in ionic liquid [Emim][N(CN)₂]/water system. *Electrochim Acta* 247:281–287
26. Tomita Y, Teruya S, Koga O, Hori Y (2000) Electrochemical reduction of carbon dioxide at a platinum electrode in acetonitrile-water mixtures. *J Electrochem Soc* 147(11):4164
27. Hara K, Sakata T (1997) Large current density CO₂ reduction under high pressure using gas diffusion electrodes. *Bull Chem Soc Jpn* 70(3):571–576
28. Jones J-P, Prakash GKS, Olah GA (2014) Electrochemical CO₂ reduction: recent advances and current trends. *Isr J Chem* 54(10):1451–1466
29. Fischer F, Prziza O (1914) Über die elektrolytische Reduktion von unter Druck gelöstem Kohlendioxyd und Kohlenoxyd. *Ber Dtsch Chem Ges* 47(1):256–260
30. Hara K, Kudo A, Sakata T (1995) Electrochemical reduction of carbon dioxide under high pressure on various electrodes in an aqueous electrolyte. *J Electroanal Chem* 391(1):141–147
31. Hara K, Tsuneto A, Kudo A, Sakata T (1994) Electrochemical reduction of CO₂ on a Cu electrode under high pressure: factors that determine the product selectivity. *J Electrochem Soc* 141(8):2097–2103
32. Li J, Prentice G (1997) Electrochemical synthesis of methanol from CO₂ in high-pressure electrolyte. *J Electrochem Soc* 144(12):4284–4288

33. Ramdin M, Morrison ART, de Groen M, van Haperen R, de Kler R, van den Broeke LJP, Trusler JPM, de Jong W, Vlught TJH (2019) High pressure electrochemical reduction of CO₂ to formic acid/formate: a comparison between bipolar membranes and cation exchange membranes. *Ind Eng Chem Res* 58(5):1834–1847
34. Ramdin M, Morrison ART, de Groen M, van Haperen R, de Kler R, Irtem E, Laitinen AT, van den Broeke LJP, Breugelmans T, Trusler JPM, Jong WD, Vlught TJH (2019) High-pressure electrochemical reduction of CO₂ to formic acid/formate: effect of pH on the downstream separation process and economics. *Ind. Eng. Chem. Res.* 58(51):22718–22740
35. Endrödi B, Kecsenovity E, Samu A, Darvas F, Jones RV, Török V, Danyi A, Janáky C (2019) Multilayer electrolyzer stack converts carbon dioxide to gas products at high pressure with high efficiency. *ACS Energy Lett.* 4:1770–1777
36. Proietto F, Schiavo B, Galia A, Scialdone O (2018) Electrochemical conversion of CO₂ to HCOOH at tin cathode in a pressurized undivided filter-press cell. *Electrochim Acta* 277:30–40
37. Scialdone O, Galia A, Nero GL, Proietto F, Sabatino S, Schiavo B (2016) Electrochemical reduction of carbon dioxide to formic acid at a tin cathode in divided and undivided cells: effect of carbon dioxide pressure and other operating parameters. *Electrochim Acta* 199:332–341
38. Dufek EJ, Lister TE, Stone SG (2014) Sampling dynamics for pressurized electrochemical cells. *J Appl Electrochem* 44(7):849–855
39. Dufek EJ, Lister TE, Stone SG, McIlwain ME (2012) Operation of a pressurized system for continuous reduction of CO₂. *J Electrochem Soc* 159(9):F514–F517
40. Todoroki M, Hara K, Kudo A, Sakata T (1995) Electrochemical reduction of high pressure CO₂ at Pb, Hg and In electrodes in an aqueous KHCO₃ solution. *J Electroanal Chem* 394(1):199–203
41. Kasian O, Li T, Mingers AM, Schweinar K, Savan A, Ludwig A, Mayrhofer K (2021) Stabilization of an iridium oxygen evolution catalyst by titanium oxides. *J Phys: Energy* 3(3):034006
42. Gu X-K, Camayang JCA, Samira S, Nikolla E (2020) Oxygen evolution electrocatalysis using mixed metal oxides under acidic conditions: challenges and opportunities. *J Catal* 388:130–140
43. Branch J, Alibouri M, Cook DA, Richardson P, Bartlett PN, Mátéfi-Tempfli M, Mátéfi-Tempfli S, Bampton M, Cookson T, Connell P, Smith D (2017) plastic reactor suitable for high pressure and supercritical fluid electrochemistry. *J Electrochem Soc* 164(6):H375–H381
44. Reference electrodes influence electrochemical measurements. <https://www.gamry.com/application-notes/instrumentation/reference-electrodes/>.
45. Proietto F, Berche F, Galia A, Scialdone O (2021) Electrochemical conversion of pressurized CO₂ at simple silver-based cathodes in undivided cells: study of the effect of pressure and other operative parameters. *J Appl Electrochem* 51:267–282
46. Bernt M, Schröter J, Möckl M, Gasteiger HA (2020) Analysis of gas permeation phenomena in a PEM water electrolyzer operated at high pressure and high current density. *J Electrochem Soc* 167(12):124502
47. Sartory M, Wallnöfer-Ogris E, Salman P, Fellinger T, Justl M, Trattner A, Klell M (2017) Theoretical and experimental analysis of an asymmetric high pressure PEM water electrolyser up to 155 bar. *Int J Hydrogen Energy* 42(52):30493–30508
48. Kuhl KP, Cave ER, Abram DN, Jaramillo TF (2012) New insights into the electrochemical reduction of carbon dioxide on metallic copper surfaces. *Energy Environ Sci* 5(5):7050–7059
49. Panderlii JE, Ren D, Yeo BS (2017) Practices for the collection and reporting of electrocatalytic performance and mechanistic information for the CO₂ reduction reaction. *Cataly. Sci. Technol.* 7(24):5820–5832
50. Möller T, Scholten F, Thanh TN, Sinev I, Timoshenko J, Wang X, Jovanov Z, Glied M, RoldanCuenya B, Varela AS, Strasser P (2020) Electrocatalytic CO₂ reduction on cuox nanocubes: tracking the evolution of chemical state, geometric structure, and catalytic selectivity using operando spectroscopy. *Angew. Chem. Int. Ed.* 59(41):17974–17983
51. Pavesi D, Ali FSM, Anastasiadou D, Kallio T, Figueiredo M, Gruter G-JM, Koper MTM, Schouten KJP (2020) CO₂ electroreduction on bimetallic Pd–In nanoparticles. *Catal Sci Technol* 10(13):4264–4270
52. Dufek EJ, Lister TE, McIlwain ME (2011) Bench-scale electrochemical system for generation of CO and syn-gas. *J Appl Electrochem* 41(6):623–631

Publisher's Note Springer Nature remains neutral with regard to jurisdictional claims in published maps and institutional affiliations.

Authors and Affiliations

Andrew R. T. Morrison^{1,2,3} · Nandalal Girichandran¹ · Quincy Wols¹ · Ruud Kortlever¹ 

✉ Ruud Kortlever
r.kortlever@tudelft.nl

¹ Process & Energy Department, Faculty of Mechanical, Maritime and Materials Engineering, Large-Scale Energy Storage, Delft University of Technology, Leeghwaterstraat 39, 2628 CB, Delft, The Netherlands

² Present Address: Electrochemical Innovation Lab, University College London, London WC1E 7JE, UK

³ Present Address: The Faraday Institution, Didcot OX11 0RA, UK